

Supporting Information

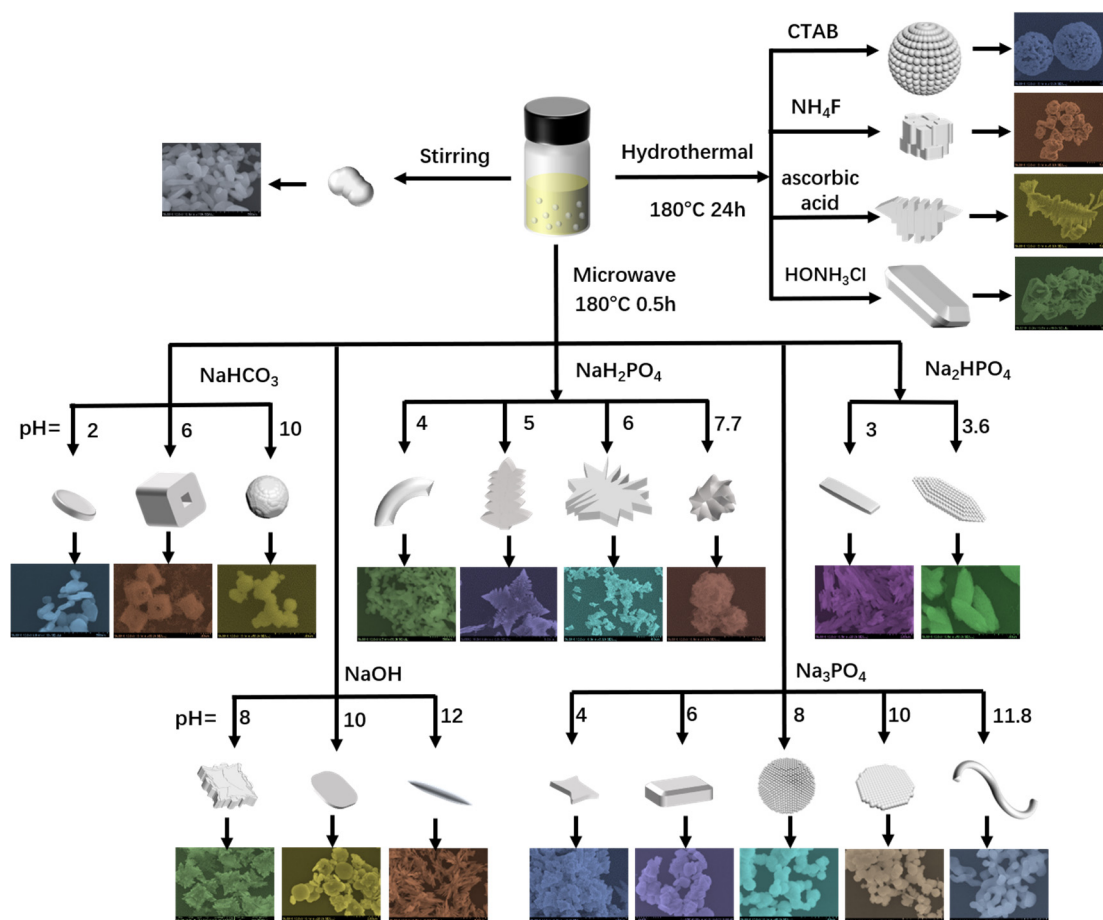


Figure S1. The synthesis produces of morphology-dependent BiVO_4 by stirring, hydrothermal and micro wave methods.

The BiVO_4 powders were synthesis by stirring, hydrothermal and micro wave methods, respectively. As a control sample, the nanoparticle BiVO_4 was prepared by stirring 30 min with the mixture of $\text{Bi}(\text{NO}_3)_3$ and NH_4VO_4 . Beside, the hydrothermal approach also used as a reference experimental method. The hexadecyl trimethyl ammonium bromide (CTAB, Sigma-Aldrich, $\geq 99\%$), NH_4F (Sigma-Aldrich, $\geq 99.99\%$), L-ascorbic acid (TCI, $>99.0\%$) and HONH_3Cl (Skychy Group, AR) were used as surfactant

to obtain the different morphology of BiVO_4 (sphere, cube, irregular and cuboid shapes). As a short time and efficient preparation method, the microwave approach can shorten the preparation time effectively, from 24 hours to 30 minutes. The morphology of BiVO_4 can be controlled with different additives, including NaH_2PO_4 , Na_2HPO_4 , Na_3PO_4 , Na_2CO_3 and NaOH . The pH values of solution from 2 to 10 were further adjusted by adding HCl or NaOH . Due to the difference in ionization and hydrolysis of phosphate, carbonate and alkaline, the morphology of bismuth vanadate could form many different shapes, including nanosheet, tetrahedron, cuboid, sphere and irregular shapes.

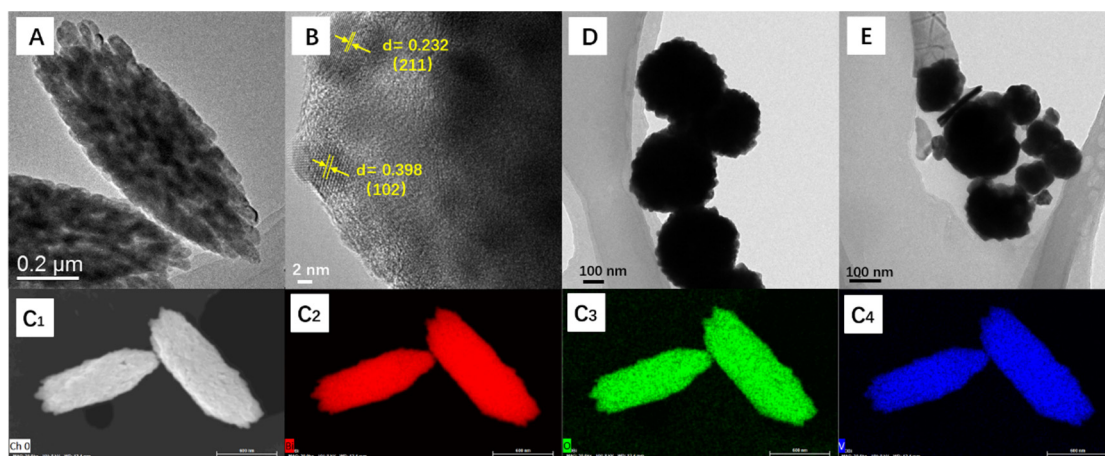


Figure S2. (A) TEM, (B) HRTEM and EDS mapping images of fusiform BiVO_4 . TEM images of (D) flowered and (E) particle BiVO_4 .

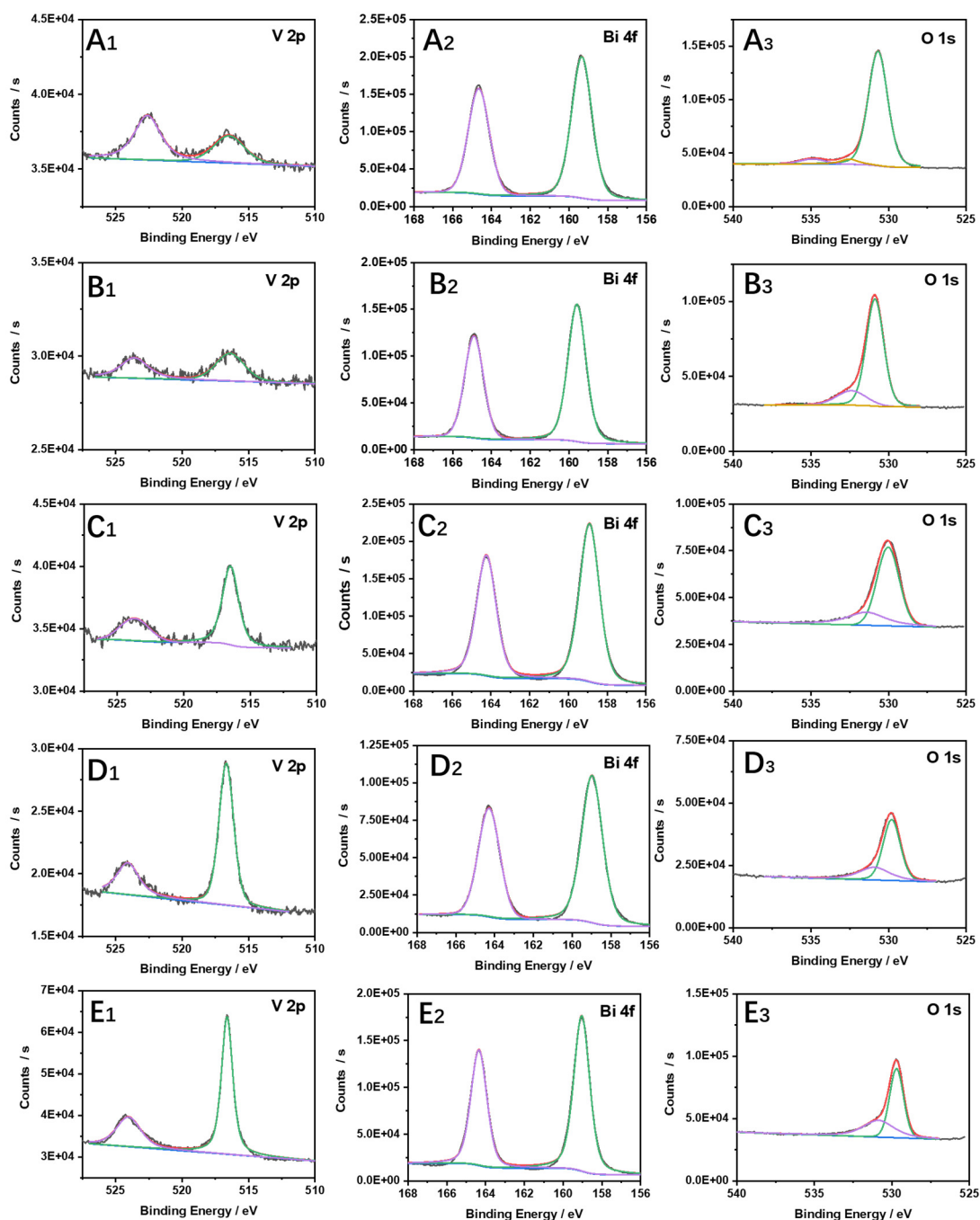


Figure S3. High-resolution XPS spectra of V 2p, Bi 4f and O 1s. (A) clavate (B) fusiform (C) flowered, (D) bulky and (E) particle BiVO_4 .

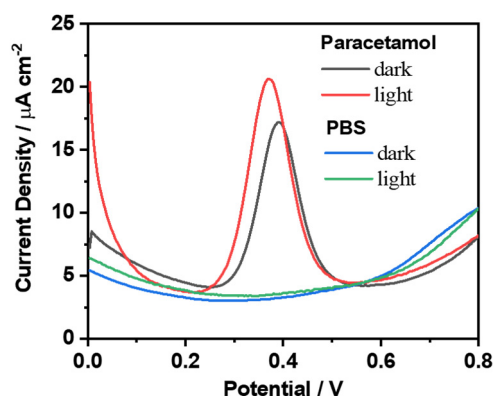


Figure S4. DPV curves of clavate BiVO_4 in 0.01 M PBS with and without 100 μM paracetamol. The DPV test was performance under dark condition (labeled as dark) and in illumination condition (labeled as light).

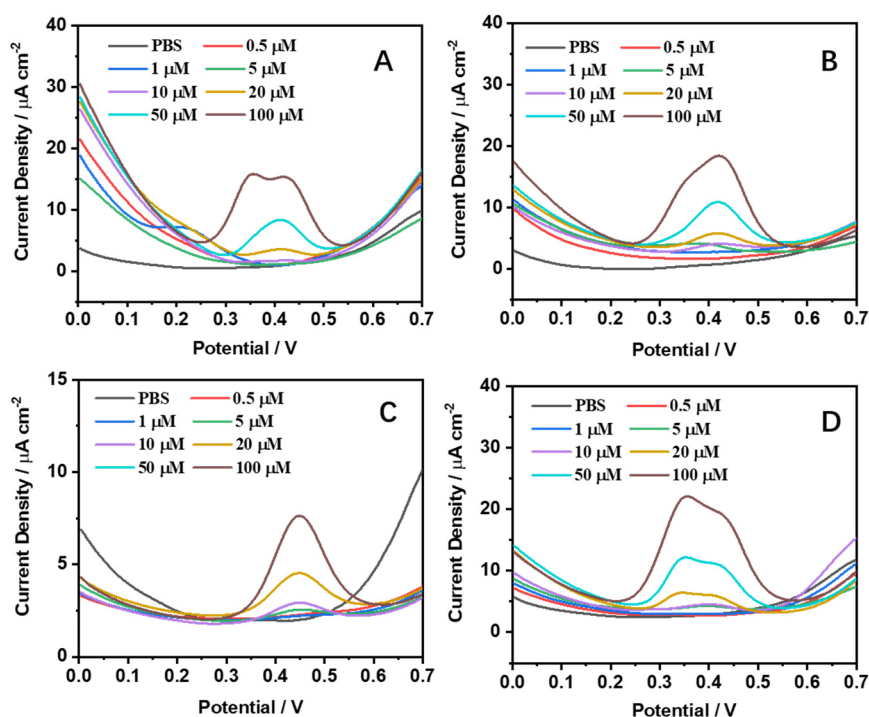


Figure S5. DPV curves at (A) fusiform (B) flowered, (C) bulky and (D) particle BiVO_4 in 0.01 M PBS with 0-100 μM paracetamol.

Table S1. Comparison between the present work and some reported sensors for paracetamol determination.

| Sensor | Solution | Linear range | LOD | Ref. |
|---|---------------------------|---------------------------------------|--------------|------|
| MWCNTs/GO | 0.05 M PBS (pH 7.0) | 0.5-400 mM | 47 nM | [1] |
| Au NPs | PBS (pH 7.4) | 0.05-270 μ M | 14.6 nM | [2] |
| Au@graphene/ PEDOT | PBS (pH 7.0) | 0.15-5.88 mM | 41 nM | [3] |
| TiO ₂ -graphene | 0.1 M PBS 0.2 (pH 7.0) | 1-100 μ M | 0.21 μ M | [4] |
| Co/MWCNTs | 0.1 M PBS | 5.2×10^{-3} -0.45 μ M | 1.0 nM | [5] |
| Pd/GO | 0.1 M PBS (pH 6.8) | 0.005-0.5 μ M 0.5-80.0 μ M | 2.2 nM | [6] |
| PS-PNIPAm- PS/MWCNTs- COOH/N- GQDs | 0.1 M PBS 0.2 (pH 7.0) | 0.1-7.0 μ M 7.0-103.0 μ M | 66 nM | [7] |
| Polymeric micelle | PBS solution (pH 7.0) | 1×10^{-3} - 4 m M | 0.33 μ M | [8] |
| g-C ₃ N ₄ /PANI/ CdO | 0.1 M PBS (pH 7.4) | 0.1-790 mM | 26 μ M | [9] |
| Au-Ag | 0.2 M PBS solution | 0.01-0.1 mM | 2.6 μ M | [10] |
| NiAl LED | 0.1 M acetate buffer | 3-1500 μ M | 0.8 μ M | [11] |
| CoFe ₂ O ₄ | 0.1 M phosphate | 3-200 μ M | 250 nM | [12] |

| buffer (pH 6.0) | | | | |
|------------------------------------|---------------------------------------|------------------------|--------------------|-----------|
| NiO NPs | BR buffer (pH 3.0) | 3.0-47.8 μM | 0.12 μM | [13] |
| ZrO ₂ | PBS (pH 7.4) | 10-60 μM | 0.68 μM | [14] |
| Bi ₂ O ₃ | 0.1 M KH ₂ PO ₄ | 0.5-1500 μM | 0.2 μM | [15] |
| Fe ₂ O ₃ NPs | 0.1 M PBS (pH 7.0) | 2-170 μM | 1.16 μM | [16] |
| Clavate-BiVO ₄ | 0.01 M PBS (pH 7.4) | 0.5-100 μM | 0.2 μM | This work |

LOD: limit of detection; PBS: phosphate buffer saline; BR buffer: Britton-Robison buffer; MWCNTs: multi-wall carbon nanotubes; GO: graphene oxide; PEDOT: Poly(3,4-ethylenedioxythiophene); PS-PNIPAm-PS: polymer poly(styrene-b-(N-isopropylacrylamide)-b-styrene); MWCNTs-COOH: carboxylated multi-walled carbon nanotubes; N-GQDs: amino-functionalized graphene quantum dots.

References

1. X. Kang, J. Wang, H. Wu, J. Liu, I. A. Aksay, Y. Lin, A graphene-based electrochemical sensor for sensitive detection of paracetamol, *Talanta* 2010, 3, 754-759.
2. N. F. Atta, A. Galal, S. M. Azab, Electrochemical determination of paracetamol using gold nanoparticles-application in tablets and human fluids, *Int. J. Electrochem. Sci.* 2011, 6 5082-5096.
3. M. Li, W. Wang, Z. Chen, Z. Song, X. Luo, Electrochemical determination of paracetamol based on Au@graphene core-shell nanoparticles doped conducting polymer PEDOT nanocomposite, *Sens. Actuat. B-Chem.* 2018, 260, 778-785.
4. Y. Fan, J. Liu, H. Lu, Q. Zhang, Electrochemical behavior and voltammetric determination of paracetamol on Nafion/TiO₂-

graphene modified glassy carbon electrode, *Colloid. Surface. B* 2011,85, 289-292.

5. A. Kutluay, M. Aslanoglu, An electrochemical sensor prepared by sonochemical one-pot synthesis of multi-walled carbon nanotube-supported cobalt nanoparticles for the simultaneous determination of paracetamol and dopamine, *Anal. Chim. Acta* 2014, 839, 59-66
6. J. Li, J. Liu, G. Tan, J. Jiang, S. Peng, M. Deng, D. Qian, Y. Feng, Y. Liu, High-sensitivity paracetamol sensor based on Pd/graphene oxide nanocomposite as an enhanced electrochemical sensing platform, *Biosens. Bioelectron.* 2014, 54, 468-475..
7. P. Zhao, M. Ni, C. Chen, Z. Zhou, X. Li, C. Li, Y. Xie, J. Fei, Stimuli-enabled switch-like paracetamol electrochemical sensor based on thermosensitive polymer and MWCNTs-GQDs composite nanomaterial, *Nanoscale* 2019, 11, 7394-7403.
8. J. Luo, C. Fan, X. Wang, R. Liu, X. Liu, A novel electrochemical sensor for paracetamol based on molecularly imprinted polymeric micelles, *Sensor. Actuat. B-Chem* 2013,188,909-916.
9. S. Bonyadi, K. Ghanbari, M. Ghiasi, All-electrochemical synthesis of a three-dimensional mesoporous polymeric g-C₃N₄/PANI/CdO nanocomposite and its application as a novel sensor for the simultaneous determination of epinephrine, paracetamol, mefenamic acid, and ciprofloxacin, *New J. Chem.* 2020, 44, 3412.
10. R. Wei, Biosynthesis of Au–Ag alloy nanoparticles for sensitive electrochemical determination of paracetamol, *Int. J. Electrochem. Sci.* 2017, 12, 9131-9140.

11. K. Asadpour-Zeynali, R. Amini, Nanostructured hexacyanoferrate intercalated Ni/Al layered double hydroxide modified electrode as a sensitive electrochemical sensor for paracetamol determination, *Electroanalysis* 2017, 29, 635-642.
12. Y. Kumar, P. Pramanik, D. K. Das, Electrochemical detection of paracetamol and dopamine molecules using nano-particles of cobalt ferrite and manganese ferrite modified with graphite, *Heliyon*, 2019, 5, e02031.
13. P. B. Deroco, F. C. Vicentini, O. Fatibello-Filho, An electrochemical sensor for the simultaneous determination of paracetamol and codeine using a glassy carbon Electrode modified with nickel oxide Nanoparticles and carbon black, *Electroanalysis* 2015, 27, 2214-2220.
14. S. B. Matt, S. Raghavendra, M. Shivanna, M. Siddlinganahalli, D. M. Siddalingappa, Electrochemical detection of paracetamol by voltammetry techniques using pure zirconium oxide nanoparticle based modified carbon paste electrode, *J. Inorg. Organomet. P.* 2020, doi.org/10.1007/s10904-020-01743-y.
15. M. Zidan, T. W. Tee, A. H. Abdullah, Z. Zainal, G. J. Kheng, Electrochemical oxidation of paracetamol mediated by nanoparticles bismuth oxide modified glassy carbon Electrode, *Int. J. Electrochem. Sci.* 2011, 6, 279-288.
16. M. M. Vinay, Y. A. Nayaka, Iron oxide (Fe_2O_3) nanoparticles modified carbon paste electrode as an advanced material for electrochemical investigation of paracetamol and dopamine, *J. Sci-Adv. Mater. Dev.* 2019, 4, 442-450.